Fixed Point of the Finite System DMRG

Hiroshi Takasaki, Toshiya Hikihara,[1*] and Tomotoshi Nishino[2**]

Department of Physics, Graduate School of Science and Technology, Kobe University, Rokkodai 657-8501
[1]*Division of Information and Media Science, Graduate School of Science and Technology, Kobe University, Rokkodai 657-8501*
[2]*Department of Physics, Faculty of Science, Kobe University, Rokkodai 657-8501*

(Received)

The density matrix renormalization group (DMRG) is a numerical method that optimizes a variational state expressed by a tensor product. We show that the ground state is not fully optimized as far as we use the standard finite system algorithm, that uses the block structure $\mathbf{B}\bullet\bullet\mathbf{B}$. This is because the tensors are not improved directly. We overcome this problem by using the simpler block structure $\mathbf{B}\bullet\mathbf{B}$ for the final several sweeps in the finite iteration process. It is possible to increase the numerical precision of the finite system algorithm without increasing the computational effort.

KEYWORDS: Density Matrix, Finite System Algorithm, Fixed Point

Establishment of the density matrix renormalization group (DMRG) by White[1)] is one of the major progresses in computational condensed matter physics. DMRG enables us to calculate ground states of relatively large scale one-dimensional (1D) quantum systems.[2–6)] Two-dimensional (2D) classical systems,[7–10)] and 1D quantum system at finite temperature[11–14)] have also been investigated.

Östlund and Rommer[15)] examined the thermodynamic limit ($N \to \infty$) of the infinite system algorithm, and they pointed out that the block state $\mathbf{B}$ corresponds to a product of position independent tensor. It should be noted that their result does not show that the infinite system algorithm creates a translationally invariant — position independent — variational state for the whole system $\mathbf{B}\bullet\bullet\mathbf{B}$, where "$\bullet$" denotes a bare spin variable between the left and the right blocks. Actually, the variational state has a slight position dependence. For example, the bond energy $\langle\bullet\bullet\rangle$ at the center of the antiferromagnetic $S = 1/2$ Heisenberg chain, which is calculated by the infinite system algorithm, is lower than the exact ground state energy per site.[16)] Such a position dependence in the variational state spoils the numerical efficiency of the infinite system algorithm.[17)] As we show in the following, the finite system algorithm does not fully improve the variational state in the same reason. The purpose of this paper is to remove the source of such a numerical error, and to increase the numerical precision in DMRG.

Let us briefly review the construction of the variational state, which is used in the standard finite system algorithm. We consider the IRF model[18)] as a reference system, whose transfer matrix is written as the product of local Boltzmann weights

$$T^{s'_1 \dots s'_N}_{s_1 \dots s_N} = W^{s'_1 s'_2}_{s_1 s_2} W^{s'_2 s'_3}_{s_2 s_3} \cdots W^{s'_{N-1} s'_N}_{s_{N-1} s_N} , \qquad (1)$$

where W represents the IRF weight. The finite system algorithm, that uses the block structure $\mathbf{B}\bullet\bullet\mathbf{B}$, approximates the eigenvector of the transfer matrix using a variational state in the tensor product

$$V^{(M)}_{s_1 \dots s_N} = \sum_{\xi_2 \cdots \xi_{N-1}}^{\text{at most } m} A^{s_2}_{s_1 \xi_2} \cdots A^{s_{M-1}}_{\xi_{M-2} \xi_{M-1}} \tilde{V}^{s_M \ s_{M+1}}_{\xi_{M-1} \xi_{M+2}} B_{\xi_{M+2}}{}^{s_{M+2}}{}_{\xi_{M+3}} \cdots B_{\xi_{N-1}}{}^{s_{N-1}}{}_{s_N} , \qquad (2)$$

where $\xi_2 \cdots \xi_{N-1}$ denote m-state block spin variables. (Fig. 1(a)) The tensors $A^{s_i}_{\xi_{i-1}\xi_i}$ and $B_{\xi_j}{}^{s_j}{}_{\xi_{j+1}}$ are dependent on their positions i and j, and each of them satisfies the orthogonal relation

$$\sum_{\xi_{i-1} s_i} A^{s_i}_{\xi_{i-1}\xi_i} A^{s_i}_{\xi_{i-1}\xi'_i} = \delta_{\xi_i \xi'_i}$$

$$\sum_{s_j \xi_{j+1}} B_{\xi_j}{}^{s_j}{}_{\xi_{j+1}} B_{\xi'_j}{}^{s_j}{}_{\xi_{j+1}} = \delta_{\xi_j \xi'_j} , \qquad (3)$$

where we have written s_1 and s_N as ξ_1 and ξ_N, respectively. Normally, they impose the normalization[19)]

$$\sum_{\xi_{M-1} s_M s_{M+1} \xi_{M+2}} \left(\tilde{V}^{s_M \ s_{M+1}}_{\xi_{M-1} \xi_{M+2}} \right)^2 = 1 . \qquad (4)$$

The standard finite system algorithm improves the variational state (eq. (2)) so that (Fig. 1(b))

$$\lambda^{(M)} = \sum_{\text{all indices}} V^{(M)}_{s'_1 \dots s'_N} T^{s'_1 \dots s'_N}_{s_1 \dots s_N} V^{(M)}_{s_1 \dots s_N} \qquad (5)$$

is maximized via the tuning of $\tilde{V}^{s_M \ s_{M+1}}_{\xi_{M-1} \xi_{M+2}}$, under the constraint eq. (4). The best $\tilde{V}^{s_M \ s_{M+1}}_{\xi_{M-1} \xi_{M+2}}$ is determined by

* E-mail: hikihara@phys.sci.kobe-u.ac.jp
** E-mail: nishino@phys.sci.kobe-u.ac.jp

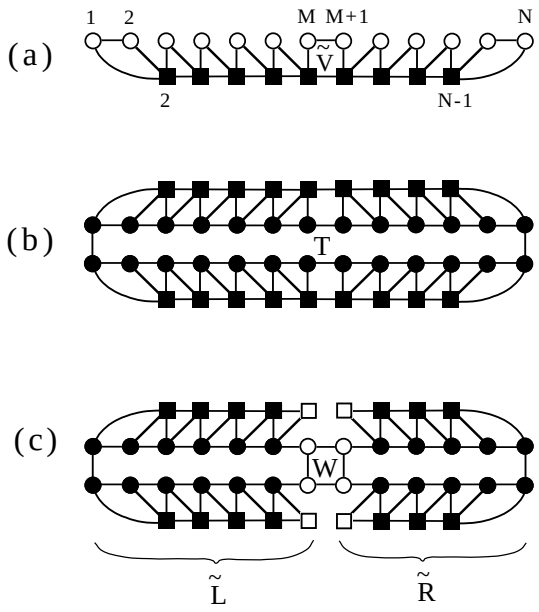

Fig. 1. Graphical representation of (a) the variational state, (eq. (2)) (b) the variational eigenvalue of the transfer matrix, (eq. (5)) and (c) the renormalized transfer matrix. (eq. (6)) Circles and squares denote bare and renormalized spin variables, respectively. We use black marks when the variables are summed up in the corresponding equations.

the diagonalization of the renormalized transfer matrix

$$\tilde{T}^{\xi'_{M-1}s'_M s'_{M+1}\xi'_{M+2}}_{\xi_{M-1}s_M s_{M+1}\xi_{M+2}} = \tilde{L}^{\xi'_{M-1}s'_M}_{\xi_{M-1}s_M} W^{s'_M s'_{M+1}}_{s_M s_{M+1}} \tilde{R}^{s'_{M+1}\xi'_{M+2}}_{s_{M+1}\xi_{M+2}}, \tag{6}$$

and by identifying its eigenvector $\tilde{V}_{\xi_{M-1}s_M s_{M+1}\xi_{M+2}}$ with the tensor $\tilde{V}^{s_M\ s_{M+1}}_{\xi_{M-1}\xi_{M+2}}$. The factor $\tilde{L}^{\xi'_{M-1}s'_M}_{\xi_{M-1}s_M}$ and $\tilde{R}^{s'_{M+1}\xi'_{M+2}}_{s_{M+1}\xi_{M+2}}$ represent the renormalized half-row transfer matrix for the left and the right half of the system, respectively. (Fig. 1(c)) A pair of tensors $A^{s_M}_{\xi_{M-1}\xi_M}$ and $B_{\xi_{M+1}\xi_{M+2}}^{\ \ s_{M+1}}$ are then improved *indirectly* by rewriting the improved tensor $\tilde{V}^{s_M\ s_{M+1}}_{\xi_{M-1}\xi_{M+2}}$ using the singular value decomposition (SVD)

$$\tilde{V}^{s_M\ s_{M+1}}_{\xi_{M-1}\xi_{M+2}} = \sum_{\xi_M\xi_{M+1}}^{2m} A^{s_M}_{\xi_{M-1}\xi_M}\, \Omega_{\xi_M\xi_{M+1}}\, B_{\xi_{M+1}\xi_{M+2}}^{\ \ s_{M+1}}, \tag{7}$$

and by restricting the degree of freedom of ξ_M and ξ_{M+1} down to m. The matrix $\Omega_{\xi_M\xi_{M+1}}$ is a $2m$-dimensional diagonal matrix[20]

$$\Omega = \begin{pmatrix} \omega_1 & & & \\ & \omega_2 & & \\ & & \ddots & \\ & & & \omega_{2m} \end{pmatrix}, \tag{8}$$

where the diagonal elements are in the decreasing order $|\omega_1| \geq |\omega_2| \geq \cdots |\omega_{2m}|$. The matrix Ω satisfies the normalization $\mathrm{Tr}\,\Omega^2 = \sum_\xi^{2m} \omega_\xi^2 = 1$. The finite system algorithm improves other tensors in eq. (2) by shifting the position of $\tilde{V}$ by use of the wave function renormalization.[21,22]

In the above standard improvement process for the variational state $V^{(M)}_{s_{1\cdots}s_N}$, the tensors $A^{s_M}_{\xi_{M-1}\xi_M}$ and $B_{\xi_{M+1}\xi_{M+2}}^{\ \ s_{M+1}}$ are improved indirectly, only through the tuning for $\tilde{V}^{s_M\ s_{M+1}}_{\xi_{M-1}\xi_{M+2}}$. As a result, $A^{s_M}_{\xi_{M-1}\xi_M}$ and $B_{\xi_{M+1}\xi_{M+2}}^{\ \ s_{M+1}}$ are determined under the condition where $2m$ degrees of freedom is allowed for both ξ_M and ξ_{M+1}, although only m states are allowed for other block spin variables $\xi_2 \cdots \xi_{M-1}$ and $\xi_{M+2} \cdots \xi_N$. It is apparent that additional m numbers of freedom is allowed at the position where $\tilde{V}$ is. (This excess freedom is common to both the finite and the infinite system algorithms.) Thus the variational state $V^{(M)}_{s_{1\cdots}s_N}$ is dependent on M, even after many sweeps of the finite system process. Figure 2 shows $\ln\left(\lambda^{(M)}\right)$ of the square lattice Ising model of the width $N = 200$ with free boundary condition, where we define the local Boltzmann weight as

$$W^{s'_i s'_{i+1}}_{s_i s_{i+1}} = \exp\left\{\frac{K}{2}(s'_i s'_{i+1} + s_i s_{i+1} + s_i s'_i + s'_{i+1} s_{i+1} - 4)\right\} \tag{9}$$

for the Ising spins $s = \pm 1$. We keep $(m =)8$ states for the block spins.[23] We have chosen the critical temperature $K = J/k_{\mathrm{B}}T_{\mathrm{c}}$. Since $2m$ degrees of freedom is allowed for both ξ_M and ξ_{M+1}, the eigenvalue $\lambda^{(M)}$ of the renormalized transfer matrix $\tilde{T}^{\xi'_{M-1}s'_M s'_{M+1}\xi'_{M+2}}_{\xi_{M-1}s_M s_{M+1}\xi_{M+2}}$ is dependent on M; $\lambda^{(M)}$ takes its maximum when $M = N/2$.

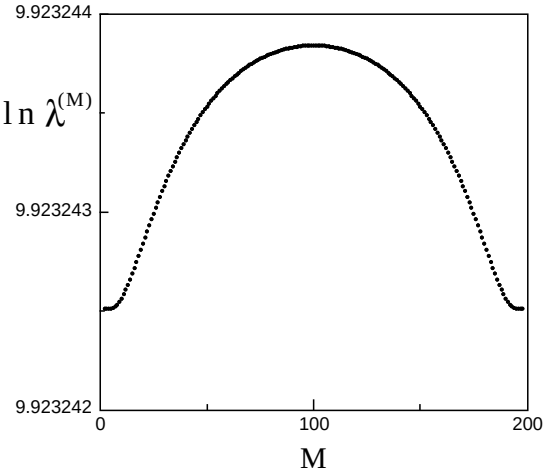

Fig. 2. The logarithm of $\lambda^{(M)}$, which is the eigenvalue of the renormalized transfer matrix $\tilde{T}^{\xi'_{M-1}s'_M s'_{M+1}\xi'_{M+2}}_{\xi_{M-1}s_M s_{M+1}\xi_{M+2}}$ of the Ising model at the critical temperature when $N = 200$ and $m = 8$. Open boundary condition is chosen.

The M dependence of the variational state $V^{(M)}_{s_{1\cdots}s_N}$ causes an ambiguity for the observation of local quantities. For example, they calculate the local magnetization of the Ising model using the formulation

$$\langle s_M \rangle = \sum_{s_{1\cdots}s_N} V^{(M)}_{s_{1\cdots}s_N}\, s_M\, V^{(M)}_{s_{1\cdots}s_N} \tag{10}$$

$$= \sum_{\xi_{M-1} s_M s_{M+1} \xi_{M+2}} \tilde{V}^{s_M \ s_{M+1}}_{\xi_{M-1} \xi_{M+2}} \ s_M \ \tilde{V}^{s_M \ s_{M+1}}_{\xi_{M-1} \xi_{M+2}} ,$$

and therefore $\langle s_M \rangle$ and $\langle s_{M'} \rangle$ for $M \neq M'$ are calculated for *different* variational states $V^{(M)}_{s_{1\cdots} s_N}$ and $V^{(M')}_{s_{1\cdots} s_N}$, respectively. The way to avoid such an ambiguity is simply to obtain a variational state that is independent on M.

Now we show that we can further improve the variational state using the block structure $\mathbf{B} \bullet \mathbf{B}$, and that the improved variational state is not dependent on M. The block structure $\mathbf{B} \bullet \mathbf{B}$ is known from the establishment of DMRG,[1,24] but the difference between $\mathbf{B} \bullet \bullet \mathbf{B}$ and $\mathbf{B} \bullet \mathbf{B}$ has not been investigated from the view point of the numerical precision. In this case, the renormalized transfer matrix is constructed as

$$\tilde{T}^{\xi'_{M-1} s'_M \xi'_{M+1}}_{\xi_{M-1} s_M \xi_{M+1}} = \tilde{L}^{\xi'_{M-1} s'_M}_{\xi_{M-1} s_M} \tilde{R}^{s'_M \xi'_{M+1}}_{s_M \xi_{M+1}} , \qquad (11)$$

where the improvement for the variational state is performed via the diagonalization of this $2m^2$-dimensional matrix. The eigenvector $\tilde{U}_{\xi_{M-1} s_M \xi_{M+1}}$ of the transfer matrix (eq. (11)) is $2m^2$-dimensional, and it is possible to rewrite it as[22]

$$\begin{aligned} \tilde{U}_{\xi_{M-1} s_M \xi_{M+1}} &= \sum_{\xi_M}^{m} A^{s_M}_{\xi_{M-1} \xi_M} \Omega'_{\xi_M \xi_{M+1}} \\ &= \sum_{\xi_M}^{m} \Omega'_{\xi_{M-1} \xi_M} B_{\xi_M}^{\ \ s_M}{}_{\xi_{M+1}} \end{aligned} \qquad (12)$$

using the Gramm-Schmidt orthogonalization; $A^{s_M}_{\xi_{M-1} \xi_M}$ and $B_{\xi_M}^{\ \ s_M}{}_{\xi_{M+1}}$ are orthogonal matrices that satisfy eq. (3), and $\Omega'_{\xi_{M-1} \xi_M}$ and $\Omega'_{\xi_M \xi_{M+1}}$ are m-dimensional diagonal matrices. (Note that in general $\Omega'_{\xi_{M-1} \xi_M}$ is not equal to $\Omega'_{\xi_M \xi_{M+1}}$.) Therefore, to use the block structure $\mathbf{B} \bullet \mathbf{B}$ in the finite system algorithm is equivalent to write down the variational state using the tensor product (Fig. 3)

$$\begin{aligned} U^{(M)}_{s_{1\cdots} s_N} = \sum_{\xi_2 \cdots \xi_{N-1}}^{\text{at most } m} & A^{s_2}_{s_1 \xi_2} \cdots A^{s_M}_{\xi_{M-1} \xi_M} \Omega'_{\xi_M \xi_{M+1}} \\ & B_{\xi_{M+1}}^{\ \ s_{M+1}}{}_{\xi_{M+2}} \cdots B_{\xi_{N-1}}^{\ \ s_{N-1}} , \end{aligned} \qquad (13)$$

and to improve $A^{s_M}_{\xi_{M-1} \xi_M}$ and $B_{\xi_M}^{\ \ s_M}{}_{\xi_{M+1}}$ *directly* via diagonalization of $\tilde{T}^{\xi'_{M-1} s'_M \xi'_{M+1}}_{\xi_{M-1} s_M \xi_{M+1}}$. All block spins $\xi_2 \cdots \xi_{N-1}$ are at most m-state; this is the non-negligible difference between $U^{(M)}_{s_{1\cdots} s_N}$ in eq. (13) and $V^{(M)}_{s_{1\cdots} s_N}$ in eq. (2).

Since $\xi_2 \cdots \xi_{N-1}$ are less than m-state in $U^{(M)}_{s_{1\cdots} s_N}$, (eq. (13)) we keep all the non-zero eigenvalues of the density matrix during the numerical calculation of the finite system algorithm; we don't cut off any states. As we repeat the improvement for the tensors $A^{s_i}_{\xi_{i-1} \xi_i}$ and $B_{\xi_j}^{\ \ s_j}{}_{\xi_{j+1}}$ for all i and j, the variational state $U^{(M)}_{s_{1\cdots} s_N}$ gradually approaches to its fixed point $U_{s_{1\cdots} s_N}$, *which is not dependent on* M. As a result, unlike $\lambda^{(M)}$ in eq. (5), the

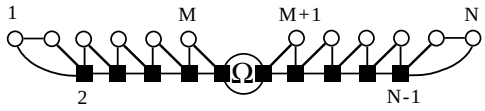

Fig. 3. The graphical representation of the variational state $U^{(M)}_{s_{1\cdots} s_N}$ defined in eq. (13). The finite system algorithm for $\mathbf{B} \bullet \mathbf{B}$ gradually improves the state, and finally $U^{(M)}_{s_{1\cdots} s_N}$ lose the M dependence.

expectation value

$$\begin{aligned} \lambda' &= \sum_{\text{all indices}} U_{s'_{1\cdots} s'_N} \, T^{s'_{1\cdots} s'_N}_{s_{1\cdots} s_N} \, U_{s_{1\cdots} s_N} \\ &= \sum_{\text{all indices}} \tilde{U}_{\xi'_{M-1} s'_M \xi'_{M+1}} \, \tilde{T}^{\xi'_{M-1} s'_M \xi'_{M+1}}_{\xi_{M-1} s_M \xi_{M+1}} \, \tilde{U}_{\xi_{M-1} s_M \xi_{M+1}} \end{aligned} \qquad (14)$$

is not dependent on M. Figure 4 shows $\ln(\lambda')$ of the Ising model; we use the same system size and parameter as those in Fig. 2. As we have expected, λ' calculated from eq. (14) does not show any M dependence. It should be noted that λ' is always larger than $\lambda^{(M)}$, which is shown for comparison. Since both $\lambda^{(M)}$ and λ' are variational lower bound for the partition function per row (= unit transfer), it is apparent that λ' is better than $\lambda^{(M)}$ in this case.

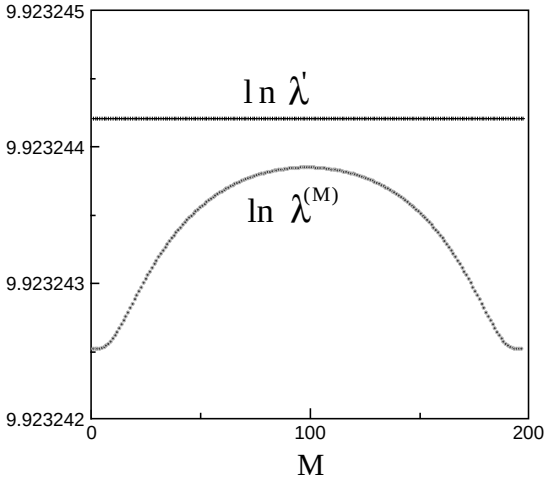

Fig. 4. The logarithm of λ', which is the eigenvalue of $\tilde{T}^{\xi'_{M-1} s'_M \xi'_{M+1}}_{\xi_{M-1} s_M \xi_{M+1}}$ for the Ising model at the critical temperature when $N = 200$ and $m = 8$. Unlike $\ln\left(\lambda^{(M)}\right)$ shown for comparison, $\ln(\lambda')$ shown by circles does not show any M dependence.

We have used the block structure $\mathbf{B} \bullet \mathbf{B}$ to obtain λ' after we calculated $\lambda^{(M)}$ using the standard block structure $\mathbf{B} \bullet \bullet \mathbf{B}$.[25] The additional calculation for $\mathbf{B} \bullet \mathbf{B}$ is not time consuming at all, because the matrix dimension of $\tilde{T}^{\xi'_{M-1} s'_M \xi'_{M+1}}_{\xi_{M-1} s_M \xi_{M+1}}$ in eq. (11) is smaller than $\tilde{T}^{\xi'_{M-1} s'_M s'_{M+1} \xi'_{M+2}}_{\xi_{M-1} s_M s_{M+1} \xi_{M+2}}$ in eq. (6), and the finite system pro-

cess can be done very rapidly with the use of the wave function renormalization.[21,22] Thus, treating $\mathbf{B} \bullet \mathbf{B}$, one can increase the numerical precision in DMRG without increasing computational time so much.

One might insist that the difference between $V^{(M)}_{s_{1\cdots}s_N}$ in eq. (2) and $U_{s_{1\cdots}s_N}$ in eq. (13) is negligible if m is sufficiently large. The statement is correct. We have to keep in mind, however, that occasionally people are suffering from increasing m in order to keep numerical precision. It is worth improving DMRG *without* increasing m,[26,27] because to keep large m is difficult for complicated models.

It is straightforward to introduce the $\mathbf{B} \bullet \mathbf{B}$ structure to the infinite system algorithm in order to recover the translational invariance of the variational state in the thermodynamic limit. The way is, as we have done for the finite system algorithm, first to employ the block structure $\mathbf{B} \bullet \bullet \mathbf{B}$ and to perform the infinite RG processes till the renormalized wave function converges,[28] and then to use $\mathbf{B} \bullet \mathbf{B}$ to perform additional infinite processes. In this way, the translationally invariant variational state by Östlund-Rommer[15] is obtained numerically via DMRG.

We thank K. Okunishi and Y. Hieida for discussions about the tensor product formulation. We also thank to S. R. White, G. Sierra, X. Wang, T. Xiang, E. Carlon and I. Peschel for valuable discussion at the Max-Planck-Institute für Physik komplexer System in Dresden. We thank T. Tonegawa for providing us IBM RISC station type 560 and 595 for this research.

1) S. R. White: Phys. Rev. Lett. **69** (1992) 2863; S. R. White: Phys. Rev. **B 48** (1993) 10345.
2) S. R. White and D. A. Huse: Phys. Rev. **B48** (1993) 3844.
3) E. S. Sorensen and I. Affleck: Phys. Rev. Lett **71** (1993) 1633; E. S. Sorensen and I. Affleck: Phys. Rev. **B49** (1994) 15771.
4) N. Shibata, A. Tsvelik and K. Ueda: Phys. Rev. **B 56** (1997) 330.
5) G. A. Gehring, R. J. Bursill and T. Xiang: Acta Phys. Pol. **A91** (1997) 105.
6) G. Sierra and M. A. Martín-Delgado: *Strongly Correlated Magnetic and Superconducting Systems,* (Springer Berlin, 1997), and references there in.
7) T. Nishino: J. Phys. Soc. Jpn. **64** (1995) 3598.
8) Enrico Carlon and Andrzej Drzewiński: Phys. Rev. Lett. **79** (1997) 1591; Enrico Carlon and Andrzej Drzewiński: Phys. Rev. **E57** (1998) 2626.
9) Enrico Carlon and Ferenc Igloi: Phys. Rev. **B 57** (1998) 7877; Ferenc Igloi and Enrico Carlon: cond-mat/9805083.
10) Enrico Carlon, Andrzej Drzewiński and Jos Rogiers: Phys. Rev. **B58** (1998) 5070.
11) R. J. Bursill, T. Xiang, G. A. Gehring: J. Phys. Condensed Matter **40** (1996) L583.
12) X. Wang and T. Xiang: Phys. Rev. **B56** (1997) 5061.
13) N. Shibata: J. Phys. Soc. Jpn **66** (1997) 2221.
14) Sebastian Eggert and Stefan Rommer: Phys. Rev. Lett. **81** (1998) 1690.
15) S. Östlund and S. Rommer: Phys. Rev. Lett **75** (1995) 3537; S. Rommer and S. Östlund: Phys. Rev. **B55** (1997) 2164.
16) The fact does not contradict to the variational principle in DMRG. The bond energy except at the center of the system is higher than the true energy per site, thus the variational principle is not violated.
17) J. Dukelsky, M. A. Martín-Delgado, T. Nishino and G. Sierra: Europhys. Lett. **43** (1998) 457.
18) R. J. Baxter: *Exactly Solved Models in Statistical Mechanics* (Academic Press, London, 1982).
19) We have assumed that the transfer matrix is symmetric. For an asymmetric transfer matrix, we have to prepare the dual pair ($\sim$ conjugate) of $\tilde{V}$.[7,12,13,18]
20) Precisely speaking, Ω does not have to be diagonal. We have shown the simplest case.
21) S. R. White: Phys. Rev. Lett. **77** (1996) 3633.
22) T. Nishino and K. Okunishi: J. Phys. Soc. Jpn. **64** (1995) 4084.
23) We choose such a small m in order to clearly visualize the M-dependence in $\lambda^{(M)}$.
24) The $\mathbf{B} \bullet \mathbf{B}$ structure has been employed for the DMRG in momentum space. See T. Xiang: Phys. Rev. **B53** (1996) 10445.
25) One should not use $\mathbf{B} \bullet \mathbf{B}$ at the early stage in the finite system algorithm.[1]
26) M.-B. Lepetit and G. M. Pastor: cond-mat/9809233.
27) R. J. Bursill: cond-mat/9812349.
28) The convergence in variational state is much slower than the convergence in local energy. See M. Andersson, M. Boman and S. Östlund: cond-mat/9810093.